Percutaneous endoscopic lumbar partial laminectomy assisted by a new miniature parallel surgical robot system: a trial on a cadaveric specimen

Nan Su[1*], Jiashen Shao[1*], Gang Zhu[2], Yu Wang[3,4]

1 Department of Orthopedics, Beijing Friendship Hospital, Capital Medical University, Beijing, China
2 Beijing Rossum Robot Co., Ltd, Beijing, China
3 School of Biological Science and Medical Engineering, Beihang University, Beijing, China
4 Beijing Advanced Innovation Center for Biomedical Engineering, Beihang University, Beijing, China

KEY WORDS

cadaveric specimen, percutaneous lumbar laminectomy, preoperative planning, spinal endoscopy, surgical robot

ABSTRACT

INTRODUCTION Robot-assisted surgery is becoming increasingly popular and its application is expanding to various spinal surgical procedures, including endoscopic spinal surgery.

AIM The aim of this study was to describe a novel small parallel orthopedic surgical robot and evaluate its feasibility in assisting surgeons during percutaneous lumbar laminectomy on cadaveric specimens.

MATERIALS AND METHODS The authors of the study developed a new orthopedic surgical navigation system (R-Pharos, Rossum Robot Co., Ltd, Beijing, China), consisting of a navigation cart and a hybrid serial-parallel bedside robotic arm. The system is equipped with interactive software for selecting and planning the percutaneous lumbar laminectomy target and path. A cadaveric specimen was selected for a right-side partial laminectomy at L4. During the procedure, the surgeon used the robotic arm to guide the saw to the target lamina and perform the percutaneous resection. Postoperative cone beam computed tomography (CBCT) and endoscopic assessments were used to confirm the resection outcome.

RESULTS After optimizing the precision of the small parallel orthopedic surgical robot to 1 mm, it was shown to meet the navigational requirements for percutaneous lumbar laminectomy. The surgeon utilized the interactive software to design the resection range and path for the right L4 lamina which was successfully resected, as confirmed by endoscopic observation. A postoperative CBCT scan revealed that the resection area precisely matched the preoperative design.

CONCLUSIONS This study demonstrated that the small parallel orthopedic surgical robot was capable of preoperatively planning the lamina resection area and could assist the surgeon in performing percutaneous lumbar laminectomy with high navigational precision.

Correspondence to:
Nan Su, MD, Department of Orthopedics, Beijing Friendship Hospital, Capital Medical University, 95 of Yong'an Road, Xicheng, 100050 Beijing, China, phone: +86 13391936034, email: 898988619@qq.com
Received: December 8, 2024.
Revision accepted: February 28, 2025.
Published online: March 24, 2025.
Wideochir Inne Tech Maloinwazyjne. 2025; 20 (1): 99-105
doi:10.20452/wiitm.2025.17935
Copyright by the Authors, 2025

* NS and JS contributed equally to this work.

INTRODUCTION Lumbar spinal stenosis (LSS) is a type of degenerative lumbar disease that leads to neurogenic claudication and is often accompanied by lower back pain.[1] Since the early 1980s, when spinal endoscopy started being used to treat lumbar disc disease,[2] this field has been developing rapidly. Unilateral laminectomy for bilateral decompression (ULBD) surgery is a common minimally invasive lumbar decompression procedure performed using spinal endoscopy to treat LSS. Compared with traditional open lumbar decompression surgery, its advantages include a smaller incision, less damage to soft tissues and paraspinal muscles, less bleeding, shorter hospital stays, and faster patient recovery. However, performing ULBD with spinal endoscopy requires high surgical skills. The key to successful surgery is the correct placement of the working channel of the spinal endoscope at the target decompression site, which helps shorten the operation time and prevents intraoperative complications. This step requires

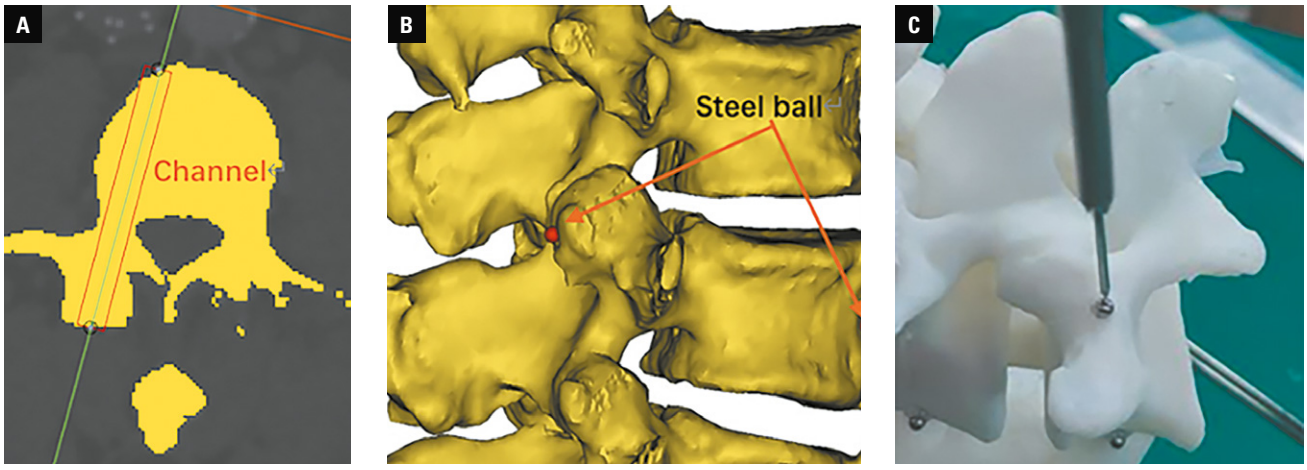

FIGURE 1 Precision test procedure. The channel indicates as pedicle screw was drawn on computed tomography (CT) scan imaging (**A**). Two ends of the channel: the foci of the channel and the facet, and the channel and the anterior edge of vertebral body, were marked (**B**). We made a 3-dimensional printing model according to the CT data and placed the steel balls on it. A joint-type 3-dimentional coordinate measuring machine was used to measure the straight-line distance from the steal balls to the central axis of the gauge (**C**).

significant surgical experience, making the ULBD learning curve quite steep.[3]

In the past decade, robot-assisted spine surgery has achieved significant success. Robotic systems can provide precise positioning guidance and execute preoperative plans. Numerous studies have shown that robot-assisted pedicle screw placement improves accuracy and reduces intraoperative radiation exposure compared with traditional manual techniques.[4-6] By adjusting software and upgrading the design of the manipulator, orthopedic robots can also assist in lumbar decompression surgery, particularly in guiding endoscopic lumbar laminotomy. With robotic assistance and other instruments, surgeons can perform bone decompression operations such as laminectomy and partial resection of the facet. Subsequently, an endoscope can be inserted to carry out soft tissue decompression, including, among others, flavectomy or discectomy. This approach optimizes the surgical process of endoscopic lumbar spinal decompression.

We designed a new miniature parallel surgical robot system. Using this robot, we assisted surgeons in performing partial lumbar laminectomy through percutaneous channels on cadaveric specimens, aiming to explore its potential use in endoscopic lumbar laminectomy.

AIM The aim of this study was to describe a novel small parallel orthopedic surgical robot and evaluate its feasibility in assisting surgeons during percutaneous lumbar laminectomy on cadaveric specimens.

MATERIALS AND METHODS **Robot design** In this study, we used a new orthopedic surgical navigation system (R-Pharos, Rossum Robot Co., Ltd, Beijing, China). The system consists of 2 parts: the navigation cart, which includes surgical tool navigation system and a human-machine interface (HMI), and the manipulator. The navigation cart is used for patient image registration. The HMI allows surgeons to set the decompression channel on the image. The manipulator is partially used to execute accurate movements. The manipulator used in this study is a series-parallel hybrid manipulator bedside connection system. The weight of the manipulator system is 12.5 kg, and its arm span is 800 mm. It is directly fixed to the surgical bed via a bedside rail.

The series part is a custom-made passive control system with 5 joints and 9 degrees of freedom, capable of handling a 15 kg load. It can be manually dragged and locked in any position. The parallel part is a miniaturized Stewart platform that can provide small-range, 6-degree-of-freedom movements within a 30 mm diameter cylinder. The upper part of the Stewart platform features a special joint that connects either the guide or the phantom to the optical position sensor.

At the end of the parallel structure, there is a display that shows the direction of the normal plane of the guide. The display moves along with the parallel structure. This screen connects to a computer via Bluetooth, allowing real-time monitoring of the projected coordinates of the planned screw head and tail on the normal plane of the guide. By moving the end structure and aligning the screw head and tail on the screen, the rough desired position is achieved. Once the operator locks the position, the parallel structure ensures precise placement. Compared with a fixed monitor, this movable display better reflects the positional relationship between the end guide and the spatial screw channel, making it easier for the operator to achieve the desired rough position.

During the procedure, we first securely connected the manipulator to the surgical bed and attached a 3-dimensional phantom to the end of the manipulator. Next, we installed a tracker at the posterior inferior iliac spine to serve as the global reference point. By releasing the passive

TABLE 1 Results of the precision test in the first lumbar model

Entry point of each level	Precision, mm	Removal point of each level	Precision, mm
L1	0.654	L1	1.049
L2	0.518	L2	1.002
L3	0.879	L3	1.000
L4	0.560	L4	1.130
L5	1.080	L5	1.050
R1	0.880	R1	1.068
R2	0.631	R2	0.946
R3	0.688	R3	0.580
R4	0.660	R4	0.750
R5	0.880	R5	0.650

Abbreviations: L, left; R, right

TABLE 2 Results of the precision test in the second lumbar model

Entry point of each level	Precision, mm	Removal point of each level	Precision, mm
L1	0.528	L1	0.794
L2	0.530	L2	0.680
L3	0.270	L3	0.320
L4	0.770	L4	0.970
L5	0.610	L5	0.760
R1	0.770	R1	0.970
R2	1.110	R2	0.830
R3	1.030	R3	1.030
R4	0.210	R4	0.520
R5	1.010	R5	1.160

Abbreviations: see **TABLE 1**

control system, the 3-dimensional phantom was positioned above the specimen's spine. We then used cone beam computed tomography (CBCT) scanning to complete the registration.

The surgeons planned the desired screw trajectory on the registration image of the spine. After planning, we removed the 3-dimensional phantom and installed the guide. The passive control system moved the guide to the position close to the target vertebra and locked it in place. At this point, the platform precisely aligned with the planned screw trajectory. The surgeons could then insert the gauge along the guide's direction. Once the gauge reached the bone surface, the surgeons drilled the K-wire into the vertebral body and completed pedicle screw placement along the K-wire.

Verification of precision CT models of the lumbar spine and pelvis from 2 patients were used for 3-dimensional reconstruction and 3-dimensional printing. The surgeon designed the trajectory of the pedicle screw and drew a channel from the facet to the anterior edge of vertebral body. The 2 end points of this channel (entry point and removal point) were marked. To verify the precision of the system, we installed a steel ball in each point for each vertebral segment and a tracker at the posterior inferior iliac spine in the 3-dimensional printing model. During the precision test, we found the position of the steel ball in the CT 3-dimensional reconstruction model and moved the robotic arm to the ideal position. Then, we used a joint-type 3-dimensional coordinate measuring machine to find the central axis coordinates of the gauge and the coordinates of the steel balls, respectively. The deviation was calculated as the straight-line distance from the steal balls to the central axis of the gauge, which was represented as a system error. This procedure is illustrated in **FIGURE 1**. As there were lumbar CT scan data from 2 patients, a total of 20 pedicle channels (L1 to L5, bilaterally) were recorded and the precision was measured one by one. The results of the precision test are presented in **TABLES 1** and **2**.

Statistical analysis Data analysis was conducted using the R software (The R Foundation for Statistical Computing, Vienna, Austria). The precision of the entry and removal points is preserved to 3 significant digits.

Ethics statement The experimental protocol was reviewed and approved by the Ethics Committee of the Beijing Friendship Hospital (2022KY087).

RESULTS Cadaveric specimen simulation surgery Previous studies and cadaver research have proven that the studied spinal surgical robot could assist during pedicle screw placement with high accuracy (**FIGURES 1** and **2**). Moreover, we explored the use of this surgical robot to navigate other spinal surgical procedures, such as partial lumbar laminectomy. Below, we describe the simulation of the robot-assisted partial lumbar laminectomy process on a cadaveric specimen.

Using a human cadaveric specimen, we performed robot-assisted percutaneous lumbar partial laminectomy, targeting the right lamina of L4. The specimen was placed in the prone position on the surgical table, with the R-Pharos miniature parallel surgical robot positioned on its right side and fixed to the surgical bedframe. After using fluoroscopy to locate L3–L5, the surgeon made a longitudinal incision on the surface of the L3 spinous process. The skin, subcutaneous tissue, and deep fascia were incised to expose the surface of the L3 spinous process where we placed a tracker and ensured that it could be detected by the network device interface stereo camera (optical position sensor). Through CBCT scanning of L3–L5 of the specimen, we obtained both 2- and 3-dimensional reconstructions of the vertebrae. The reconstruction model is shown in **FIGURE 3**.

Using this model, we could plan the target laminectomy site and the operation pathway. Since the surgical tool for the laminectomy was a trephine with a diameter of 0.8 cm, we used software to generate a cylinder of the same diameter and placed it in the spinal model. In the coronal section, we moved the cylinder to the junction of

FIGURE 2 A novel orthopedic surgical navigation system (R-Pharos, Rossum Robot Co., Ltd, Beijing, China) assists during pedicle screw placement.

the lower edge of the L4 lamina and the inferior articular process of L4, which was the target laminectomy site. Then, we adjusted the position of the cylinder in the sagittal plane, making it perpendicular to the lamina. By reverse stretching of the cylinder, we could determine the position of the skin incision point, which was the intersection of the cylinder with the skin. The 3-dimensional coordinates of the skin incision and the target lamina point were recorded, with the skin incision as the entry point and the target lamina point as the exit point. The design of the target laminectomy site is shown in **FIGURE 4**.

Afterwards, the surgeon moved the manipulator near the skin incision. Guided by the display on the manipulator, the surgeon adjusted the manipulator's position until the indicator light turned green, and then locked it in place. The remote platform of the manipulator was further activated to adjust the precision between the entry and exit points to within 1 mm. The surgeon then inserted the trephine along the guide, ensuring the entry point was where the trephine contacted the skin. The skin, subcutaneous tissue, and deep fascia were cut. As the trephine approached the bone surface, the surgeon confirmed that the precision was still within 1 mm, used the trephine to remove a part of the lamina, and then dismounted the trephine. The surgical procedure and the excised bone specimen of the lamina are shown in **FIGURE 5**.

Reusing the same spinal reconstruction model, we could design and plan the second laminectomy target site on the rostral side of the first target site. To avoid leaving residual lamina when using the trephine, we needed to partially overlap the second laminectomy target site with the first one to ensure that the distance between the 2 centers was less than 1.5 cm. The second target site is illustrated in **FIGURE 4**.

Since no additional incisions were needed, the original incision served as the entry point, and the second target site as the exit point, with the line connecting them representing the trephine's trajectory. We then used software to record the coordinates of each point mentioned above. The manipulator platform was activated to ensure that the precision between the entry and exit points was always within 1 mm. The surgeon

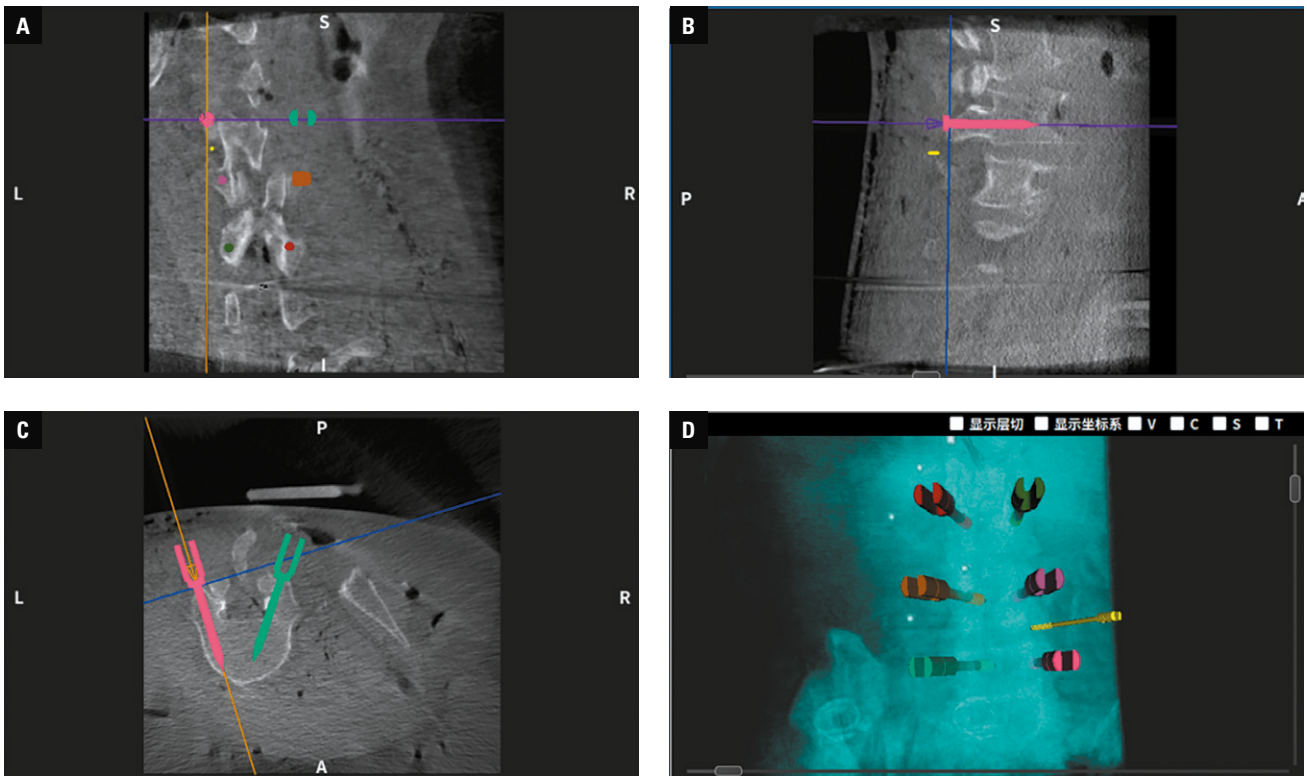

FIGURE 3 The 2-dimensional (**A**–**C**) and 3-dimensional (**D**) reconstruction models of the vertebrae obtained by cone beam computed tomography scanning of the specimens

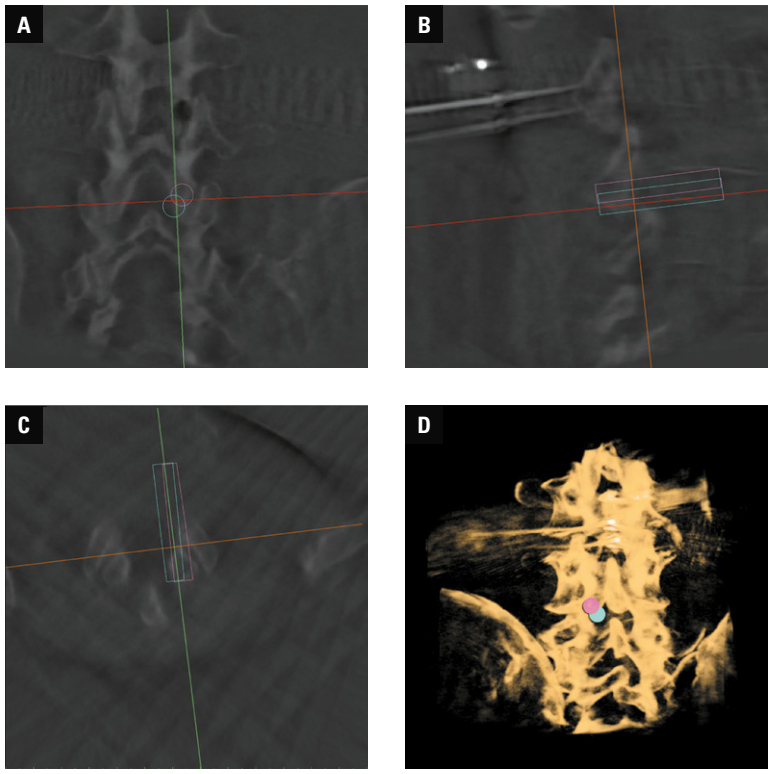

FIGURE 4 Two lamina target sites were designed by the 2- and 3-dimensional reconstruction spinal models. The figure displays coronal (**A**), sagittal (**B**), cross-sectional (**C**), and 3-dimensional reconstructed images (**D**) of the area where the target is located. Two cylinders with a 0.8 cm diameter, which represented the trephine, were generated. The first target site was located at the junction of the lower edge of the L4 lamina and the inferior articular process of L4. The second target site was on the rostral side of the first target site, overlapping partially.

FIGURE 5 The surgeon used the trephine to remove a part of the lamina with the R-Pharos miniature parallel surgical robot assistance.

then reinserted the trephine through the original incision to the second target on the lamina surface, excised part of the lamina, and removed the trephine. The precision of the entry and exit points is detailed in **TABLES 1** and **2**.

The spinal endoscope was inserted through the skin entry point. Another CBCT scan of L3–L5 of the cadaveric specimen was performed, allowing for 2- and 3-dimensional reconstructions. Through these reconstructions, we could observe the excision at the first and second target sites (**FIGURE 6**).

DISCUSSION As endoscopic spinal surgery is a widely used procedure, an increasing number of surgeons employ this technology to perform lumbar laminectomy for LSS. Unlike simple endoscopic discectomy, it is still a challenge for surgeons to use endoscopy to perform lumbar partial laminectomy, even ULBD. Compared with lumbar disc herniation (LDH) patients, individuals with LSS are elderly and suffer from more severe lumbar degeneration. The lumbar anatomical landmarks may be ambiguous as the osteophyte and hypertrophy ligaments interfere. Surgeons need more training and experience to perform the endoscopic lumbar decompression surgery for LSS than in the case of LDH.[7] The latest study shows that surgeons can overcome the learning curve after performing 35 surgeries, which is when operation time and radiation exposure decrease significantly.[8] Compared with traditional open lumbar decompression surgery, percutaneous endoscopic lumbar laminectomy (PELS) is significantly less invasive, with smaller incision, less bleeding, and better lumbar posterior muscles and ligaments protection, but it is not completely safe. Even for experienced surgeons, the complication rate for PELS is still 6%–12%, including, among others, dual tear, nerve root injury, hematoma, or insufficient decompression.[8-10]

To help surgeons overcome the learning curve, it is essential to simplify PELS procedures by enhancing positioning accuracy, reducing surgery time, and minimizing intraoperative radiation exposure. As a result, numerous new technologies have been integrated into PELS surgeries. One notable technology is the navigation system which provides real-time positioning information, enabling surgeons to precisely locate the position and depth of surgical instruments.[11] Research has demonstrated that the use of O-arms or other navigation systems facilitates accurate punctures and effective surgical path guidance during PELS procedures.[12,13] However, it does have certain drawbacks. Surgeons must concentrate on the navigation interface, making it challenging to simultaneously monitor the surgical image through the spinal endoscope. Consequently, using the navigation system requires surgeons to possess strong hand-eye coordination skills.

In recent years, the advancement of surgical robots has led to significant achievements in spinal surgery. Many studies have demonstrated that robot-assisted surgery enhances the accuracy of pedicle screw placement and reduces intraoperative radiation exposure, particularly in minimally invasive lumbar surgeries.[4-6,14] Compared with traditional navigation systems, robot-assisted surgery allows surgeons to preplan the procedure, eliminating the need for real-time monitoring of the robotic interface. Based on the success of orthopedic surgical robots in pedicle screw placement, we believe their application can be

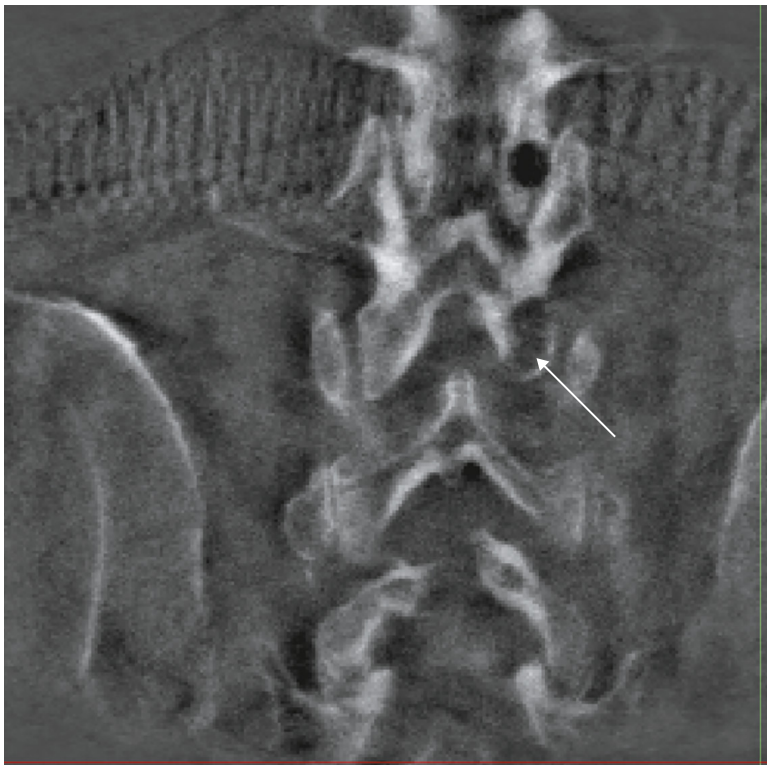

FIGURE 6 The partial bones of lamina (arrow) were precisely removed, as confirmed by the postoperative cone beam computed tomography scan and imaging reconstruction.

extended to assist with lumbar decompression surgeries under spinal endoscopy. Therefore, we developed this robotic system and applied it to assist in lumbar laminectomy.

Using the patient's lumbar CT data, surgeons can preoperatively select the target lamina resection area, design the optimal puncture path, and determine the corresponding skin incision location. In our initial trials, we successfully performed partial lumbar laminectomy on cadaver specimens with robotic assistance. By comparing preoperative and postoperative lumbar CT scans, we verified that the intraoperative lamina resection closely matched the preoperatively designed target, demonstrating high accuracy of this approach. With preoperative planning and robotic-assisted positioning, surgeons can achieve precise lamina resection, minimize unnecessary bone removal, and avoid postoperative iatrogenic spinal instability. Additionally, robotic assistance ensures that the puncture process and subsequent partial lumbar laminectomy are not compromised by abnormal anatomical landmarks or other intraoperative visual impediments, such as bleeding or bone debris from drilling. It also mitigates the impact of the surgeon's lack of experience. With robotic assistance, surgeons can minimize damage to critical anatomical structures, shorten surgery time, and reduce intraoperative radiation exposure.

There are various types of surgical instruments for endoscopic lumbar laminectomy, such as drills, piezoelectric osteotome, or trephines. Li et al[15] designed a novel spinal robot with a piezoelectric osteotome and force sensor. The robot to performed laminectomy autonomously. We believe, however, that trephines are particularly well-suited for orthopedic surgical robots because they can be easily gripped and guided by the manipulator. Unlike high-speed drills or piezoelectric osteotome, trephines perform circular rotational bone removal at a relatively low speed, making them easier forthe manipulator to control. This allows surgeons to perform bone resections accurately. Furthermore, based on preoperative lumbar CT images, surgeons can determine the thickness of the target lamina for resection. Once the trephine is activated for bone removal, the manipulator can automatically limit its depth according to the lamina thickness. The trephine features a depth gauge, allowing surgeons to observe the gauge markings through the endoscope and determine how deep the trephine has penetrated the bone. This dual-check system ensures safety during lamina resection. With a diameter of only 0.8 cm, the trephine allows surgeons to avoid unnecessary bone removal, preserve the integrity of the facet joints, and reduce the risk of postoperative iatrogenic lumbar instability. Given these advantages, we selected trephines for lamina resection and cadaveric specimen experiments.

For this study, we selected a new type of miniature parallel surgical robot and proposed an innovative serial-parallel hybrid manipulator system. This system is smaller and lighter than common manipulator platforms such as Tirobot,[16,17] Mazor X,[18] and Globus,[19] providing a spatial advantage in the operating room. Since the manipulator is fixed to the surgical bed, there is no obstruction from the platform below the bed, making it more convenient for the C-arm to capture additional fluoroscopic verification positions if needed. The small size of the manipulator also minimizes interference with the surgeon's operating area. Miniature parallel robots offer higher rigidity compared with serial robots and exhibit lower inertia during movement, allowing them to respond to the patient's breathing with smaller movements. This feature provides unique advantages for future applications, for example, in respiratory monitoring. However, as the robot is directly connected to the surgical bed, the bed needs to be more rigid. The overall rigidity of this system is slightly lower than that of platform-based manipulators. To ensure stability, surgeons need to press the gauge against the bone surface before drilling.

In the future, robot-assisted lumbar laminectomy could bring significant transformative changes. It allows the manipulator to guide the direction and orientation of the surgical tool (such as the trephine) while simultaneously limiting its depth. In theory, when working with this method, the surgeons can even use the trephine to perform percutaneous laminectomy with robotic assistance. In this approach, they do not need to insert the endoscope and rely on its imaging. Once the bone resection is completed, the spinal

endoscope can be used for further procedures, such as ligamentum flavum resection and discectomy, thus optimizing the process of spinal endoscopic surgery.

This study has some limitations. First of all, we simulated PELS surgery using a cadaveric specimen. In cadaveric specimens, there is no interference in the surgical field caused by bleeding or muscle tension affecting the precision of the manipulator's movements. Secondly, the CBCT scan of the lumbar region does not provide a high-resolution image for spinal reconstruction. Finally, robot-assisted spinal endoscopic surgery requires an additional skin incision to expose the spinous process and place the tracker. In future studies, we need to further adjust the design of the surgical robot to meet the requirements for assisting lumbar decompression surgery under spinal endoscopy.

CONCLUSIONS Following precision optimization to 1 mm, the parallel orthopedic robotic system demonstrated compliance with navigational standards for percutaneous lumbar laminectomy. Utilizing interactive planning software, the right L4 lamina resection path was executed successfully, with endoscopic and CBCT confirmation of complete consistency between intraoperative outcomes and the preoperative design. This validates the system's capability for high-precision preoperative planning and intraoperative navigation in laminectomy procedures.

ARTICLE INFORMATION

ACKNOWLEDGMENTS The authors would like to thank all the staff participating in this study.

FUNDING This study was supported by Beijing Natural Science Foundation (grant no. L222057; to NS).

CONTRIBUTION STATEMENT NS and JS made substantial contributions to the concept of the work. NS and JS made contributions to the acquisition and analysis of data. NS and JS drafted the manuscript. GZ helped with data management and statistical analysis. YW helped to critically revise the manuscript for important intellectual content. All authors approved the final version to be published. All data for this study are available upon request from the corresponding author(s).

AI STATEMENT Artificial intelligence was not used to write the article.

CONFLICT OF INTEREST None declared.

OPEN ACCESS This is an Open Access article distributed under the terms of the Creative Commons Attribution 4.0 International License (CC BY 4.0), allowing anyone to copy and redistribute the material in any medium or format and to remix, transform, and build upon the material, including commercial purposes, provided the original work is properly cited.

HOW TO CITE Su N, Shao J, Zhu G, Wang Y. Percutaneous endoscopic lumbar partial laminectomy assisted by a new miniature parallel surgical robot system: a trial on a cadaveric specimen. Wideochir Inne Tech Maloinwazyjne. 2025; 20: 99-105. doi:10.20452/wiitm.2025.17935

REFERENCES

1 Phillips FM, Slosar PJ, Youssef JA, et al. Lumbar spine fusion for chronic low back pain due to degenerative disc disease: a systematic review. Spine (Phila Pa 1976). 2013; 38: E409-E422.

2 Huang X, Liu X, Zhu B, et al. Evaluation of augmented reality surgical navigation in percutaneous endoscopic lumbar discectomy: clinical study. Bioengineering (Basel). 2023; 10: 1297.

3 Choi DJ, Choi CM, Jung JT, et al. Learning curve associated with complications in biportal endoscopic spinal surgery: challenges and strategies. Asian Spine J. 2016; 10: 624-629.

4 Stull JD, Mangan JJ, Vaccaro AR, et al. Robotic guidance in minimally invasive spine surgery: a review of recent literature and commentary on a developing technology. Curr Rev Musculoskelet Med. 2019; 12: 245-251.

5 Fatima N, Massaad E, Hadzipasic M, et al. Safety and accuracy of robot-assisted placement of pedicle screws compared to conventional free-hand technique: a systematic review and meta-analysis. Spine J. 2021; 21: 181-192.

6 Keric N, Eum DJ, Afghanyar F, et al. Evaluation of surgical strategy of conventional vs. percutaneous robot-assisted spinal trans-pedicular instrumentation in spondylodiscitis. J Robot Surg. 2017; 11: 17-25.

7 Ahn Y. Percutaneous endoscopic decompression for lumbar spinal stenosis. Expert Rev Med Devices. 2014; 11: 605-616.

8 Yang J, Guo C, Kong Q, et al. Learning curve and clinical outcomes of percutaneous endoscopic transforaminal decompression for lumbar spinal stenosis. Int Orthop. 2020; 44: 309-317.

9 Hoogland T, van den Brekel-Dijkstra K, Schubert M, et al. Endoscopic transforaminal discectomy for recurrent lumbar disc herniation: a prospective, cohort evaluation of 262 consecutive cases. Spine (Phila Pa 1976). 2008; 33: 973-978.

10 Kim W, Kim SK, Kang SS, et al. Pooled analysis of unsuccessful percutaneous biportal endoscopic surgery outcomes from a multi-institutional retrospective cohort of 797 cases. Acta Neurochir (Wien). 2020; 162: 279-287.

11 Mayberg MR, LaPresto E, Cunningham EJ. Image-guided endoscopy: description of technique and potential applications. Neurosurg Focus. 2005; 19: E10.

12 Fan G, Wang C, Gu X, et al. Trajectory planning and guided punctures with isocentric navigation in posterolateral endoscopic lumbar discectomy. World Neurosurg. 2017; 103: 899-905.e894.

13 Hur JW, Kim JS, Cho DY, et al. Video-assisted thoracoscopic surgery under O-arm navigation system guidance for the treatment of thoracic disk herniations: surgical techniques and early clinical results. J Neurol Surg A Cent Eur Neurosurg. 2014; 75: 415-421.

14 Hyun SJ, Kim KJ, Jahng TA, et al. Minimally invasive robotic versus open fluoroscopic-guided spinal instrumented fusions: a randomized controlled trial. Spine (Phila Pa 1976). 2017; 42: 353-358.

15 Li Z, Jiang S, Song X, et al. Collaborative spinal robot system for laminectomy: a preliminary study. Neurosurg Focus. 2022; 52: E11.

16 Yan K, Zhang Q, Tian W. Comparison of accuracy and safety between second-generation TiRobot-assisted and free-hand thoracolumbar pedicle screw placement. BMC Surg. 2022; 22: 275.

17 Zhao C, Zhu G, Wang Y, et al. TiRobot-assisted versus conventional fluoroscopy-assisted percutaneous sacroiliac screw fixation for pelvic ring injuries: a meta-analysis. J Orthop Surg Res. 2022; 17: 525.

18 Lee NJ, Zuckerman SL, Buchanan IA, et al. Is there a difference between navigated and non-navigated robot cohorts in robot-assisted spine surgery? A multicenter, propensity-matched analysis of 2,800 screws and 372 patients. Spine J. 2021; 21: 1504-1512.

19 Wallace DJ, Vardiman AB, Booher GA, et al. Navigated robotic assistance improves pedicle screw accuracy in minimally invasive surgery of the lumbosacral spine: 600 pedicle screws in a single institution. Int J Med Robot. 2020; 16: e2054.